ACS Sustainable Chemistry & Engineering

pubs.acs.org/journal/ascecg

Research Article

Improving Carbonate-Promoted C–H Carboxylation Using Mesoporous Carbon Supports

Emma D. Chant, Chastity S. Li, and Matthew W. Kanan*

Cite This: *ACS Sustainable Chem. Eng.* 2023, 11, 5876–5882

Read Online

ACCESS | Metrics & More | Article Recommendations | Supporting Information

ABSTRACT: C–H carboxylation is an attractive way to utilize CO_2 for chemical production provided that it does not consume resource-intensive reagents. Alkali carbonates dispersed into the pores of mesoporous supports display strongly basic reactivity under CO_2, allowing them to be used as base promoters for C–H carboxylation of (hetero)arenes in the absence of other reagents or catalysts. Mesoporous oxides are convenient support materials, but only a relatively small fraction of the dispersed carbonate (ca. 10–20%) is converted to carboxylate products when metal oxide supports are used. Here, we compare mesoporous oxide and carbon supports and investigate the dependence of carbonate reactivity on the pore structure. We show that using mesoporous carbon supports can increase the carbonate conversion by 2–4× when compared to oxide supports. This improved carbonate reactivity is maintained across a variety of mesoporous carbons with different pore structures (ordered vs disordered) and pore diameters, indicating that the dispersed carbonate is intrinsically more reactive on the surface of a carbon material compared to an oxide surface. Reaction of the carboxylate products with dimethyl carbonate yields isolable methyl esters as the final product and regenerates the dispersed carbonate. We show that mesoporous carbon supports are robust to at least five cycles of successive C–H carboxylation and methylation. Understanding how the support structure affects dispersed carbonate reactivity is valuable for advancing C–H carboxylation toward practical application and utilizing these materials in other CO_2 transformations.

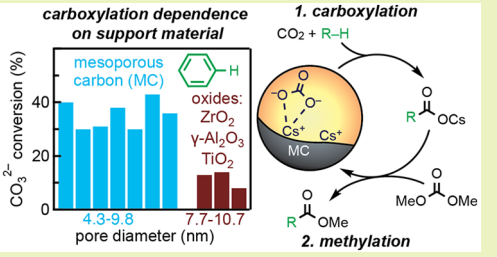

KEYWORDS: *C–H functionalization, CO_2 activation, solid base, super-basicity, mesoporous carbons, alkali carbonates*

Downloaded via STANFORD UNIV on September 18, 2023 at 21:32:03 (UTC).
See https://pubs.acs.org/sharingguidelines for options on how to legitimately share published articles.

INTRODUCTION

Utilizing CO_2 as a feedstock for chemical production is a major goal for the creation of a circular economy that minimizes non-renewable inputs.[1] C–H carboxylation, the conversion of a C–H bond into a carboxylate ($C–CO_2^-$) with CO_2 and a base (Scheme 1), has attracted interest as a way to utilize CO_2 for the preparation of carboxylic acids and their derivatives, which comprise a large number of fine and commodity chemicals.[2−6]

Scheme 1. Base-Promoted C–H Carboxylation; (a) Reaction Using a Generic Base (B^-); (b) Reaction Using CO_3^{2-}[a]

a) reaction promoted by generic base B^-

$$C–H + B^- + CO_2 \longrightarrow C–CO_2^- + BH$$

b) Carbonate-promoted C–H carboxylation

$$C–H + CO_3^{2-} + CO_2 \longrightarrow C–CO_2^- + HCO_3^-$$

$$HCO_3^- \longrightarrow \tfrac{1}{2}\,CO_3^{2-} + \tfrac{1}{2}\,H_2O + \tfrac{1}{2}\,CO_2$$

net reaction

$$C–H + \tfrac{1}{2}\,CO_3^{2-} + \tfrac{1}{2}\,CO_2 \longrightarrow C–CO_2^- + \tfrac{1}{2}\,H_2O$$

[a]Thermal decomposition of the conjugate acid HCO_3^- produces half-equivalents of CO_2, CO_3^{2-}, and H_2O, resulting in the net reaction shown in bottom row.

C–H carboxylation is conceptually appealing because it takes advantage of the oxidation state of CO_2 and avoids the limitations of other methods to synthesize carboxylic acid derivatives, such as the need to pre-install heteroatom functionality or perform harsh oxidations.[7−9] However, most C–H carboxylation methods require (super)-stoichiometric amounts of highly reactive, resource-intensive reagents to activate the C–H bond, which negates the carbon benefit of using CO_2 as a feedstock, generates large amounts of waste products, and incurs prohibitive costs for anything other than specialty chemicals. To impact sustainability, it is critical to develop alternative carboxylation methods that utilize simple reagents that can be easily regenerated.

Carbonate is an ideal base promoter for C–H carboxylation because it is produced with minimal energy input and it can be regenerated using salt splitting processes. However, carbonate is a relatively weak base in solution, and consequently its use for C–H carboxylation in solution-phase reactions has been

Received: November 21, 2022
Revised: March 20, 2023
Published: April 3, 2023

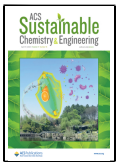

© 2023 American Chemical Society

https://doi.org/10.1021/acssuschemeng.2c06977
ACS Sustainable Chem. Eng. 2023, 11, 5876–5882

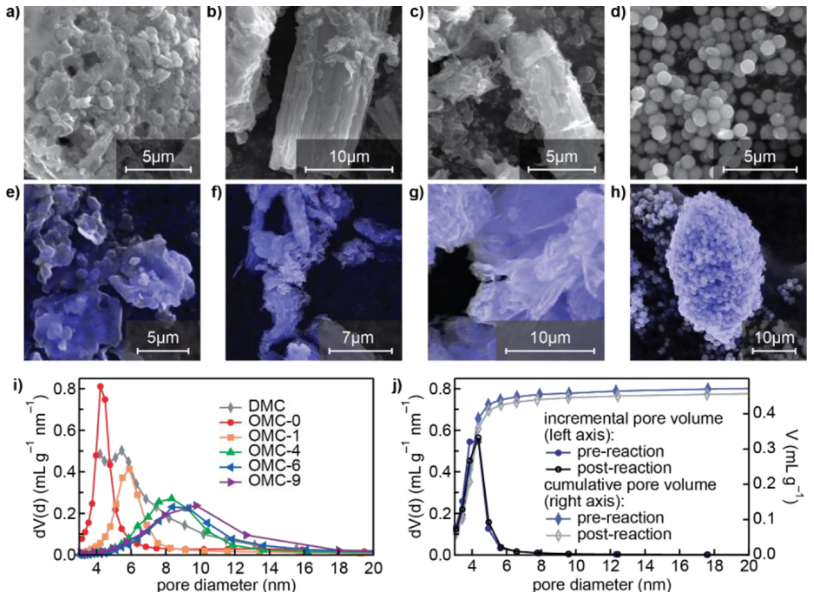

Figure 1. Characterization of mesoporous supports and Cs_2CO_3 dispersion. SEM of (a) DMC; (b) OMC-0; (c) OMC-9; and (d) TiO_2. EDS with the Cs map overlaid on SEM of (e) Cs_2CO_3/DMC; (f) Cs_2CO_3/OMC-0; (g) Cs_2CO_3/OMC-9; and (h) Cs_2CO_3/TiO_2. (i) Pore size distribution of a series of mesoporous carbon supports. (j) Pore size distribution and cumulative pore volume of Cs_2CO_3/OMC-0 before and after being used in a benzene carboxylation reaction (420 °C, 3 h). (i and j) Calculated by the desorption branch of the N_2 isotherm.

limited to substrates with pK_a ≤ 28, which includes some aromatic heterocycles.[10] Solution-phase carboxylation of higher pK_a C−H bonds requires much stronger bases and/or other resource-intensive reagents. For example, carboxylation of (benzo)thiophenes, (benzo)furans, and electron-deficient benzenes (substrates with pK_a up to ∼36)[11] has been achieved using excess LiO*t*Bu, CsF, and crown ether under a CO_2 atmosphere in an organic solvent at elevated temperatures.[12−14] C−H carboxylation of substrates with pK_a values in the high 30s or above has generally required a preliminary step to irreversibly deprotonate the C−H bond using extremely resource-intensive reagents. For example, benzene has a pK_a that is higher than what can be measured (i.e., pK_a > 40). Solution-phase C−H carboxylation of benzene has been performed using a combination of organolithium and alkoxide reagents (*n*-BuLi and KO*t*Bu),[15] zero-valent aluminum and a Lewis acid (Al^0 and $AlCl_3$),[16,17] or an alkyl Al reagent ($AlMe_{1.5}(OEt)_{1.5}$) which is effectively a methyl anion equivalent.[18] Carboxylation of high-pK_a C−H bonds that are proximal to a directing group (e.g., amide or aminoquinoline) has been demonstrated using KO*t*Bu and a transition metal catalyst to mediate C−H activation.[19] Photocatalytic methods have recently been developed to carboxylate (hetero)arene, benzylic, and styrene C−H bonds under mild conditions. These methods have broad substrate scope and can utilize carbonate as the base promoter but generally require long irradiation times and high loadings of relatively complex photosensitizers or sacrificial electron donors.[20−22]

We previously showed that alkali carbonates can serve as base promoters for high-pK_a C−H bonds when the reactions are performed in solvent-free alkali carboxylate media that form molten phases at intermediate temperatures.[23,24] This chemistry is particularly valuable for transforming monocarboxylates into dicarboxylates, as demonstrated by its use for the synthesis of furan-2,5-dicarboxylic acid.[25] More recently, we showed that alkali carbonates dispersed in mesoporous support materials can perform C−H carboxylation of aromatic hydrocarbons and heteroarenes in gas−solid reactions without using an alkali carboxylate molten salt.[26,27] Dispersion of M_2CO_3 in mesopores results in an amorphous, high surface area carbonate that deprotonates C−H bonds of gaseous reactants in the presence of CO_2, generating putative carbanion intermediates that react with CO_2 to form carboxylates. The carboxylate products can be converted into isolable methyl esters with regeneration of the dispersed alkali carbonate by reaction with methanol-saturated CO_2 or dimethyl carbonate at elevated temperatures.

We have shown that carbonate-promoted C−H carboxylation is possible with alkali carbonates dispersed in multiple types of mesoporous support materials, but little is known about how the properties of the support affect the carbonate reactivity. Mesoporous carbons are well-studied supports for heterogeneous catalysis because of their chemical and thermal stability and tunable morphologies.[28] In particular, mesoporous carbons have previously been transformed into solid base catalysts by dispersion of KNO_3 into the mesopores and thermal decomposition to generate potassium oxide sites.[29]

In this work, we systematically compare carbonates dispersed in mesoporous oxide and mesoporous carbon supports as base promoters for C−H carboxylation of benzene and benzothiophene. Benzothiophene is substantially more acidic than benzene and has a measurable pK_a of 33 in tetrahydrofuran. For a quantitative comparison, the gas-phase acidities (heterolytic bond dissociation energies) of benzene and benzothiophene are 401 kcal/mol[11,30] and 378 kcal/mol, respectively.[11] We show that for both substrates a much larger percentage of the dispersed carbonate reacts in C−H carboxylation when carbon supports are used compared to oxides. This effect is independent of the pore size and degree of pore ordering and indicates a higher intrinsic reactivity for the carbonates on the surface of the carbon supports. The carbonate reactivity shows a strong dependence on the loading for the carbon supports, however, which is a consequence of the presence of acidic functionality on the carbon surfaces.

https://doi.org/10.1021/acssuschemeng.2c06977
ACS Sustainable Chem. Eng. 2023, 11, 5876−5882

Finally, we show that carbon supports can be used in multiple cycles of C−H carboxylation followed by methylation to transform (hetero)arenes into methyl esters. The support effects on dispersed carbonate reactivity described here are important for advancing carbonate-promoted C−H carboxylation toward applications and provide insights that are valuable for other applications of dispersed carbonates such as reverse water-gas shift catalysis.[31]

RESULTS AND DISCUSSION

Support materials were prepared following reported procedures with minor modifications (see Supporting Information for full details). A highly disordered mesoporous carbon (DMC) material was prepared by pyrolyzing magnesium citrate and removing the residual MgO with HCl.[32] A series of ordered mesoporous carbon (OMC) supports with varying pore sizes were prepared by pyrolyzing sucrose solutions in SBA-15 templates and subsequently removing the templates with NaOH. The pore sizes of the OMC materials were systematically modulated by using $B(OH)_3$ to increase the SBA-15 template size.[33] These materials are designated as OMC-*X*, where *X* refers to the molar equivalents of $B(OH)_3$ used with respect to sucrose. OMC-0, with no $B(OH)_3$ added, is equivalent to CMK-3.[34] Three oxide supports were used for comparison. Mesoporous TiO_2 was synthesized by hydrolysis of titanium isopropoxide,[35] and γ-Al_2O_3 and ZrO_2 were obtained from commercial sources.

The structural properties of the supports were characterized by scanning electron microscopy (SEM) and N_2 sorption (Figures 1, S1, S2, and Table 1). The DMC support showed an irregular morphology (Figure 1a) and a large Brunauer−Emmett−Teller (BET) surface area of 1674 $m^2\ g^{-1}$. Characterization of the pore sizes by the Barrett−Joyner−Halenda (BJH) method indicated a broad distribution of pore diameters over the 3−12 nm range (Figure 1i) and a pore volume of 2.27 $cm^3\ g^{-1}$. For OMC-0, the particle shape of the SBA-15 was preserved in the templated carbon support (Figure 1b), and characterization by the BJH method indicated the expected narrow distribution of pore diameters with a maximum at 4.2 nm. This material has a lower BET surface area of 1248 $m^2\ g^{-1}$ and a pore volume of 1.64 $cm^3\ g^{-1}$. As the $B(OH)_3$ content was increased in the preparation of the OMC materials, the pore size distribution broadened and shifted to larger diameters (Figure 1i). OMC-9 (Figure 1c) exhibited a similar particle morphology to OMC-0 but with a broader pore size distribution with a maximum at 9.8 nm. Increasing the $B(OH)_3$ content past 9 equivalents further decreased the pore volume but did not increase the maximum of the distribution (Figure S2a).

Table 1. N_2 Sorption Data for Bare Supports and Cs_2CO_3 Loadings for Cs_2CO_3/Support Materials

	BET surface area of support ($m^2\ g^{-1}$)	pore volume of support ($cm^3\ g^{-1}$)	pore diameter[a] (nm)	Cs_2CO_3 loading[b] (mmol g^{-1})
DMC	1674	2.27	5.5	1.10
OMC-0	1248	1.64	4.2	0.88
OMC-0.14	1161	1.23	4.3	0.71
OMC-1	846	1.26	5.9	0.72
OMC-4	819	1.67	8.3	0.89
OMC-6	773	1.61	8.4	0.87
OMC-9	989	1.63	9.8	0.87
TiO_2	112	0.32	10.7	0.22
ZrO_2	98	0.30	7.7	0.21
γ-Al_2O_3	251	0.83	8.2	0.52

[a]The maximum of the pore size distribution plot, which was calculated by the BJH method from 77 K N_2 isotherm data (desorption branch). [b]With 0.75 M Cs_2CO_3 solution used in incipient wetness impregnation.

The metal oxide supports (TiO_2, ZrO_2, and γ-Al_2O_3) have substantially lower BET surface areas (98−251 $m^2\ g^{-1}$) and specific pore volumes (0.30−0.83 $cm^3\ g^{-1}$) compared to the carbon supports,[26] which is partly a consequence of the higher density for these materials (Table 1). At the particle level, mesoporous TiO_2 comprises regular nanospheres with ∼800 nm diameters (Figure 1d), whereas γ-Al_2O_3 and ZrO_2 were ground and sieved to form a powder with irregular, relatively large particles (Figure S3). Importantly, the pore size distributions for the oxides, with maxima between 7.7 and 10.7 nm, overlap with the high end of the range of pore sizes for the carbon supports. Thus, the oxides provide a comparison set to assess the effects of support composition (oxide vs carbon) and surface chemistry while maintaining similar pore characteristics.

The surface acidity of the mesoporous carbon supports was characterized by using Boehm's titration method.[36−38] Carbon supports were suspended in a solution of KOH in water and ethanol, which was filtered off and titrated to quantify the amount of base neutralized by the carbon. The titrations indicated a total concentration of acidic sites of 0.65 mmol g^{-1} (0.39 μmol m^{-2}) for DMC, 0.34 mmol g^{-1} (0.28 μmol m^{-2}) for OMC-0, and 0.36 mmol g^{-1} (0.36 μmol m^{-2}) for OMC-9. These values are slightly lower than several other reports of acidic sites on OMC-0, although those methods used hydrofluoric acid (HF) to remove the silica template instead of KOH.[39−41] The presence of acidic sites may be explained by re-protonation of weakly acidic species with the extensive water/methanol wash at the end of our preparation.

The support materials were loaded by the incipient wetness method using solutions of Cs_2CO_3 in methanol instead of H_2O because the hydrophobicity of the mesoporous carbon supports impedes the transport of aqueous solutions into their pores. The resulting materials are designated as Cs_2CO_3/support (support = one of the mesoporous carbon materials, TiO_2, Al_2O_3, or ZrO_2). To compare different support materials, we used a single impregnation step with a volume of 0.75 M solution of Cs_2CO_3 in methanol equal to the measured pore volume of the support material. Thus, assuming that all the pores are completely full prior to drying, this procedure results in 0.75 mmol of Cs_2CO_3 per mL of the support pore volume, which corresponds to 0.21−0.52 mmol of Cs_2CO_3 per gram of the loaded material (mmol g^{-1}) for the metal oxide supports and 0.71−1.10 mmol g^{-1} for the carbon supports (Table 1). Lower Cs_2CO_3 loadings were prepared by decreasing the concentration of the initial Cs_2CO_3 solution, and higher loadings were prepared by iterative impregnation and dying steps. Energy-dispersive X-ray spectroscopy (EDS) of DMC, OMC-0, and OMC-9 materials after Cs_2CO_3 loading showed a uniform distribution of Cs throughout the support particles, indicating that Cs_2CO_3 is well dispersed (Figure 1e−g). No bulk Cs_2CO_3 particles were observed in the SEM images. A similarly uniform Cs dispersion is observed for Cs_2CO_3 loaded into TiO_2 (Figure 1h), ZrO_2, and γ-Al_2O_3 (Figure S3).

https://doi.org/10.1021/acssuschemeng.2c06977
ACS Sustainable Chem. Eng. 2023, 11, 5876−5882

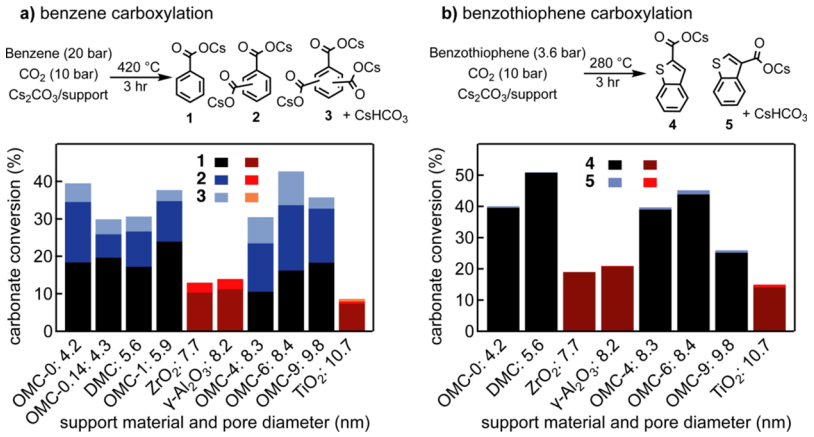

Figure 2. C−H carboxylation on carbon and oxide supports with different pore diameters. (a) Reaction scheme and conditions for benzene carboxylation and selected results. (b) General reaction scheme and conditions for benzothiophene carboxylation and selected results. The indicated pore diameters correspond to the maxima in the pore size distributions.

Loading the supports with Cs_2CO_3 reduces the specific surface area and pore volume (Figures S4 and S5). As an example, loading 1 g of OMC-0 with 0.4 g of Cs_2CO_3 (a 0.75 M loading) reduced the BET surface area from 1248 to 418 m^2 g^{-1} and the specific pore volume from 1.64 to 0.48 cm^3 g^{-1}, both greater changes than would be expected from the mass increase alone. However, the pore size distribution remained essentially the same for Cs_2CO_3/OMC-0 and the bare OMC-0 support (Figure S5a). Similar patterns were observed with Cs_2CO_3/DMC and Cs_2CO_3/OMC-9 (Figure S5b,c). When the Cs_2CO_3-loaded support was used for benzene C−H carboxylation (see below), there was no appreciable change in the pore structure after the reaction, demonstrating the stability of mesoporous carbon to carboxylation reaction conditions (Figure 1j).

C−H Carboxylation Reactions. To assess the effects of the support structure on the reactivity of dispersed Cs_2CO_3, the various dispersed carbonates were evaluated in benzene and benzothiophene C−H carboxylation reactions. For this comparison, the dispersed carbonates were all prepared using 0.75 M methanolic Cs_2CO_3 solutions to ensure that the same amount of Cs_2CO_3 was loaded per pore volume. Reactions were performed by heating a mixture of dispersed carbonate (Cs_2CO_3/support), organic substrate, and CO_2 in stainless-steel batch reactors (Figure S6). Industrial-grade CO_2 (99.5%) was used without further purification. After a specified reaction time, the reactors were cooled and depressurized, the solids were separated from the excess organic substrate, and carboxylate products were quantified by ^{1}H NMR in D_2O (Figures S7−S10). The key metric for assessing the relative reactivity of CO_3^{2-} on different supports is the CO_3^{2-} conversion—the % of Cs_2CO_3 that is consumed in C−H carboxylation to form carboxylate products. Since CO_3^{2-} has two base equivalents, 100% CO_3^{2-} conversion corresponds to 2 equivalents of carboxylates. A second metric of interest is the carboxylate yield—the amount of carboxylate products that are made per gram of the material—which determines how much material would be required to generate a desired amount of the product.

The Cs_2CO_3/carbon materials proved to be substantially more reactive than the Cs_2CO_3/oxide materials for benzene carboxylation (Figure 2a). Reactions were performed at 420 °C using a 2:1 benzene/CO_2 ratio at a total pressure of 30 bar (at 420 °C) for 3 h. The reactions produced a mixture of benzoate (**1**), phthalate isomers (**2**), and benzene tricarboxylate isomers (**3**). For Cs_2CO_3/carbon materials, the total CO_3^{2-} conversion (to all carboxylate products) ranged from 30% up to 43%, corresponding to total carboxylate yields of 345−518 μmol (benzoate + phthalate + tricarboxylate) per gram of the carbonate/support material (μmol g^{-1}). In contrast, the CO_3^{2-} conversions for Cs_2CO_3/oxide materials were only 8−14% (32−133 μmol g^{-1}). No trend was observed between the CO_3^{2-} conversion and the pore diameter of the supports. The highest CO_3^{2-} conversion (43%) was obtained with Cs_2CO_3/OMC-6, which has a similar pore size distribution as Cs_2CO_3/γ-Al_2O_3 and Cs_2CO_3/ZrO_2. These results demonstrate that the pore dimensions do not determine the reactivity of dispersed Cs_2CO_3 within the mesoscale range investigated here (4−11 nm).

In addition to higher CO_3^{2-} conversion, a higher proportion of phthalates and tricarboxylates, and thus lower selectivity for benzoate, was observed for the Cs_2CO_3/carbon materials. This result suggests that once benzoate is formed in the initial benzene C−H carboxylation, it is more reactive in the carbon material than in the oxide materials. Despite the lower selectivity of C−H carboxylation, when the Cs_2CO_3/carbon materials are used in two-step carboxylation/methylation cycles, only methyl benzoate and minor amounts of dimethyl phthalates are isolated (see below).

Substantial differences in CO_3^{2-} reactivity between carbon and oxide supports were also seen for benzothiophene carboxylation. Because of its greater acidity compared to benzene, benzothiophene reactions were performed at a lower temperature of 280 °C using a 1:2 benzothiophene/CO_2 ratio at a total pressure of 14 bar (at 280 °C) for 3 h. For all the Cs_2CO_3/support materials investigated, carboxylation occurred with ≥95% selectivity at the 2-position, which is the most acidic C−H bond of benzothiophene. A very high CO_3^{2-} conversion of 51% was obtained with Cs_2CO_3/DMC, corresponding to >1 mmol g^{-1} of the benzothiophene-2-carboxylate product. Most of the Cs_2CO_3/OMC-*X* materials showed CO_3^{2-} conversions near 40%, with somewhat lower conversion obtained with OMC-9 (Figure 2b). The reduced conversion for the latter material may be a result of some degradation of the mesoporous structure from the pore-widening procedure, as shown by the broadening of the pore size distribution (Figure 1i).

https://doi.org/10.1021/acssuschemeng.2c06977
ACS Sustainable Chem. Eng. 2023, 11, 5876−5882

In contrast to the carbon materials, substantially lower CO_3^{2-} conversions between 15 and 21% were observed for the Cs_2CO_3/oxide materials. Overall, there was no significant trend of CO_3^{2-} conversion vs the pore diameter across the mesoporous carbon and metal oxide supports. Together, the benzene and benzothiophene results demonstrate that CO_3^{2-} is intrinsically more reactive for C−H carboxylation on mesoporous supports. We postulate that the higher reactivity of Cs_2CO_3 on carbon surfaces compared to oxide surfaces is a result of a weaker Cs_2CO_3−surface interaction on the less hydrophilic carbon surfaces, which engenders greater reactivity with the gas-phase reactants.

Benzothiophene carboxylation was also used to probe the effects of Cs_2CO_3 loading on the CO_3^{2-} conversion (Figure 3).

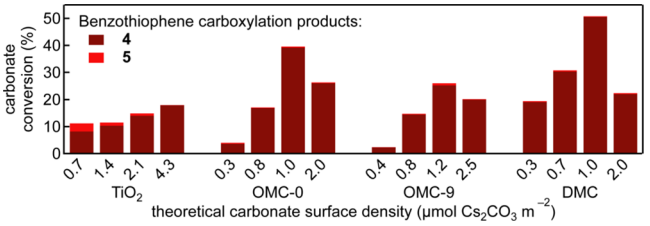

Figure 3. Effect of changing the carbonate concentration on conversion to benzothiophene carboxylation products. At low carbonate coverage, a small amount of cesium 3-carboxylate benzothiophene is formed on TiO_2, OMC-0, and OMC-9.

We examined three mesoporous carbon supports, OMC-0, OMC-9, and DMC, as well as TiO_2, and varied the Cs_2CO_3 loading between 0.25 and 1.5 M. These concentrations corresponded to a surface concentration of 0.27−2.47 μmol Cs_2CO_3 per m^2 of support (μmol m^{-2}) on the carbon supports and 0.71−4.28 μmol m^{-2} on the TiO_2 support. With the carbon supports, the CO_3^{2-} conversion showed a strong dependence on the Cs_2CO_3 loading. The lowest conversion was observed at the lowest loading, 0.25 M. At this loading, the number of surface acidic sites measured by Boehm titration (0.28−0.39 μmol/m^2) represents a substantial fraction of the amount of base equivalents loaded (2 per Cs_2CO_3 or 0.54−0.82 μmol/m^2). As the Cs_2CO_3 loading was increased, the CO_3^{2-} conversion increased, reaching a maximum at a loading of 0.75 M. Increasing the loading further to 1.5 M Cs_2CO_3, however, resulted in much lower conversions. The drop in CO_3^{2-} conversion at high loadings may indicate the formation of unreactive bulk Cs_2CO_3 domains at high loadings.[26] In contrast, the trend was much weaker on TiO_2, where increasing the loading of Cs_2CO_3 from 0.25 to 1.5 M caused a gradual increase in conversion from 10 to 20%. TiO_2 has a lower surface area and very different surface chemistry, which may affect how the carbonate is distributed and what fraction is available for reactivity. The difference in reactivity when using metal oxide supports versus mesoporous carbon supports is consistent with initial observations that residual borosilicate from the synthesis of OMC-*X* materials inhibited reactivity (Table S10).

Small amounts of carboxylation at the 3-position were observed in all benzothiophene carboxylation reactions. In the case of Cs_2CO_3/TiO_2, benzothiophene-3-carboxylate accounted for 27% of the products at 0.25 M loading, with decreasing amounts of this product as the loading was increased. The 3-position is much less acidic than the 2-position, but it is the most nucleophilic position of benzothiophene. The observation of benzothiophene-3-carboxylate at low Cs_2CO_3 loadings on TiO_2 is consistent with a separate electrophilic aromatic substitution mechanism for the carboxylation that is promoted by the TiO_2 surface. We previously observed that carboxylation at the most nucleophilic position is favored for more electron-rich heterocycles such as 1-methylindole using a variety of dispersed carbonate materials.[27] The small amounts of benzothiophene-3-carboxylate observed with DMC and OMC-0 may arise from reactivity with residual MgO and SiO_2 from the synthesis procedures.

C−H Carboxylation/Methylation Cycles. We next assessed the ability to convert carboxylate products dispersed in mesoporous carbons into isolable methyl esters and regenerate the dispersed carbonate. We previously showed that it is possible to convert arene carboxylates into methyl esters and regenerate dispersed carbonate with flowing CH_3OH-saturated CO_2 at elevated temperatures when using TiO_2 support materials. However, these conditions are not effective when mesoporous carbon supports are used or, regardless of the support material, when the methyl esters have very high boiling points. We have shown that high-boiling methyl esters on mesoporous TiO_2 can be obtained by using neat dimethyl carbonate as the methylating reagent.[27,42] We therefore evaluated these conditions for the methylation of carboxylates in mesoporous carbons (Figure 4a). We constructed a modified batch reactor with a fritted stainless-steel bottom, allowing the ester product to be washed off the mesoporous carbon without transferring the support between reactions (Figure S6). Heating the benzene carboxylate products of C−H carboxylation with mesoporous carbon supports (RCO_2Cs/MC) in neat dimethyl carbonate at 160 °C in a stainless-steel batch reactor formed the methyl ester

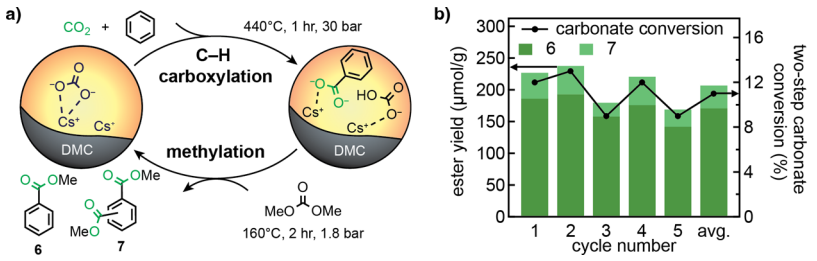

Figure 4. (a) Schematic of the esterification cycle with regeneration of dispersed carbonate on disordered mesoporous carbon (DMC). (b) Per-cycle methyl benzoate and dimethyl phthalate yields in terms of μmol ester per gram of M_2CO_3/DMC and the two-step, per-cycle, carbonate conversion for five cycles. Note that for simplicity, we have shown the species $CsHCO_3$. However, under carboxylation conditions (380−440 °C), $CsHCO_3$ is thermally unstable and will decompose back into 0.5 equivalents of Cs_2CO_3, H_2O, and CO_2.

https://doi.org/10.1021/acssuschemeng.2c06977
ACS Sustainable Chem. Eng. 2023, 11, 5876−5882

products in high yield (Figure S11). Washing the support with a dry organic solvent easily removed the esters without removing ionic species (Figure S12). Subsequent heating under vacuum resulted in regeneration of M_2CO_3/MC. Products of each cycle were quantified by high-performance liquid chromatography and averaged 171 μmol g^{-1} methyl benzoate and 36 μmol g^{-1} dimethyl phthalates (Figure 4b). Comparable yields and selectivity were maintained over five cycles of carboxylation and methylation.

CONCLUSIONS

Supported alkali carbonates are a promising reagent for CO_2 utilization as they maintain super-basicity under high CO_2 pressures. The above results demonstrate that mesoporous carbons are efficient and stable supports for Cs_2CO_3 and support higher fractions of active Cs_2CO_3 than metal oxides for the activation of weakly acidic C−H bonds in benzene and benzothiophene. Furthermore, this activity is dependent on the tunable pore volume of the supports and is robust to variation in the pore morphology. Ongoing work involves expanding the scope of CO_2 utilization reactions for alkali carbonates dispersed in mesoporous carbon supports, including their use in catalytic transformations such as the reverse water-gas shift reaction.

ASSOCIATED CONTENT

Supporting Information

The Supporting Information is available free of charge at https://pubs.acs.org/doi/10.1021/acssuschemeng.2c06977.

Additional experimental details, materials, and methods, including photographs of the experimental setup, ^{1}H NMR references for all compounds, ^{1}H NMR spectra for selected reactions, N_2 sorption data for all materials, additional reactivity data, and additional SEM images (PDF)

AUTHOR INFORMATION

Corresponding Author

Matthew W. Kanan − *Department of Chemistry, Stanford University, Stanford, California 94305, United States;* orcid.org/0000-0002-5932-6289; Email: mkanan@stanford.edu

Authors

Emma D. Chant − *Department of Chemistry, Stanford University, Stanford, California 94305, United States*

Chastity S. Li − *Department of Chemistry, Stanford University, Stanford, California 94305, United States;* orcid.org/0000-0001-7576-8362

Complete contact information is available at: https://pubs.acs.org/10.1021/acssuschemeng.2c06977

Author Contributions

E.D.C. and M.W.K. devised the project. E.D.C. performed material synthesis and reactivity studies and analyzed the results. C.S.L. performed microscopy studies. E.D.C. and C.S.L. conducted surface area and pore volume analysis. E.D.C. carried out all other characterization. E.D.C. and M.W.K. drafted the manuscript. All authors contributed to editing the manuscript.

Funding

This work was supported by the U.S. Department of Energy, Office of Science, Basic Energy Sciences under award DE-SC0020394. Part of this work was performed at the Stanford Nano Shared Facilities (SNSF), supported by the National Science Foundation under award ECCS-1542152. E.D.C. gratefully acknowledges the Center for Molecular Analysis and Design at Stanford University for fellowship support.

Notes

The authors declare no competing financial interest.

REFERENCES

(1) Artz, J.; et al. Sustainable Conversion of Carbon Dioxide: An Integrated Review of Catalysis and Life Cycle Assessment. *Chem. Rev.* **2018**, *118*, 434−504.

(2) Luo, J.; Larrosa, I. C−H Carboxylation of Aromatic Compounds through CO2 Fixation. *ChemSusChem* **2017**, *10*, 3317−3332.

(3) Ngo, H. L.; Mishra, D. K.; Mishra, V.; Truong, C. C. Recent advances in the synthesis of heterocycles and pharmaceuticals from the photo/electrochemical fixation of carbon dioxide. *Chem. Eng. Sci.* **2021**, *229*, No. 116142.

(4) Davies, J.; Lyonnet, J. R.; Zimin, D. P.; Martin, R. The road to industrialization of fine chemical carboxylation reactions. *Chem* **2021**, *7*, 2927−2942.

(5) Ran, C.-K.; Liao, L.-L.; Gao, T.-Y.; Gui, Y.-Y.; Yu, D.-G. Recent progress and challenges in carboxylation with CO2. *Curr. Opin. Green Sustainable Chem.* **2021**, *32*, No. 100525.

(6) Pimparkar, S.; et al. Recent advances in the incorporation of CO2 for C−H and C−C bond functionalization. *Green Chem.* **2021**, *23*, 9283−9317.

(7) Röhrscheid, F. Carboxylic Acids, Aromatic. In *Ullmann's Encyclopedia of Industrial Chemistry*; 2000.

(8) Ohara, T.; et al. Acrylic Acid and Derivatives. In *Ullmann's Encyclopedia of Industrial Chemistry*; 2020; pp 1−21.

(9) Kubitschke, J.; Lange, H.; Strutz, H. Carboxylic Acids, Aliphatic. In *Ullmann's Encyclopedia of Industrial Chemistry*; 2014; pp 1−18.

(10) Vechorkin, O.; Hirt, N.; Hu, X. Carbon Dioxide as the C1 Source for Direct C−H Functionalization of Aromatic Heterocycles. *Org. Lett.* **2010**, *12*, 3567−3569.

(11) Shen, K.; Fu, Y.; Li, J.-N.; Liu, L.; Guo, Q.-X. What are the pK_a values of C−H bonds in aromatic heterocyclic compounds in DMSO? *Tetrahedron* **2007**, *63*, 1568−1576.

(12) Shigeno, M.; Hanasaka, K.; Sasaki, K.; Nozawa-Kumada, K.; Kondo, Y. Direct Carboxylation of Electron-Rich Heteroarenes Promoted by LiO-tBu with CsF and [18]Crown-6. *Chem. − Eur. J.* **2019**, *25*, 3235−3239.

(13) Shigeno, M.; Sasaki, K.; Nozawa-Kumada, K.; Kondo, Y. Double-Carboxylation of Two C−H Bonds in 2-Alkylheteroarenes Using LiO-t-Bu/CsF. *Org. Lett.* **2019**, *21*, 4515−4519.

(14) Shigeno, M.; et al. Direct C−H Carboxylation Forming Polyfunctionalized Aromatic Carboxylic Acids by Combined Brønsted Bases. *Org. Lett.* **2022**, *24*, 809−814.

(15) Schlosser, M.; Jung, H. C.; Takagishi, S. Selective mono- or dimetalation of arenes by means of superbasic reagents. *Tetrahedron* **1990**, *46*, 5633−5648.

(16) Olah, G. A.; et al. Efficient Chemoselective Carboxylation of Aromatics to Arylcarboxylic Acids with a Superelectrophilically Activated Carbon Dioxide−Al 2 Cl 6 /Al System. *J. Am. Chem. Soc.* **2002**, *124*, 11379−11391.

(17) Suzuki, Y.; Hattori, T.; Okuzawa, T.; Miyano, S. Lewis Acid-Mediated Carboxylation of Fused Aromatic Compounds with Carbon Dioxide. *Chem. Lett.* **2002**, *31*, 102−103.

(18) Suga, T.; Mizuno, H.; Takaya, J.; Iwasawa, N. Direct carboxylation of simple arenes with CO 2 through a rhodium-catalyzed C−H bond activation. *Chem. Commun.* **2014**, *50*, 14360−14363.

(19) Gevorgyan, A.; Hopmann, K. H.; Bayer, A. Formal C−H Carboxylation of Unactivated Arenes. *Chem. − Eur. J.* **2020**, *26*, 6064−6069.
(20) Schmalzbauer, M.; et al. Redox-Neutral Photocatalytic C−H Carboxylation of Arenes and Styrenes with CO2. *Chem* **2020**, *6*, 2658−2672.
(21) Saini, S.; Singh, H.; Prajapati, P. K.; Sinha, A. K.; Jain, S. L. Nickel/Nickel Oxide in Combination with a Photoredox Catalyst for the Reductive Carboxylation of Unsaturated Hydrocarbons with CO2 under Visible-Light Irradiation. *ACS Sustainable Chem. Eng.* **2019**, *7*, 11313−11322.
(22) Meng, Q.-Y.; Schirmer, T. E.; Berger, A. L.; Donabauer, K.; König, B. Photocarboxylation of Benzylic C−H Bonds. *J. Am. Chem. Soc.* **2019**, *141*, 11393−11397.
(23) Banerjee, A.; Dick, G. R.; Yoshino, T.; Kanan, M. W. Carbon dioxide utilization via carbonate-promoted C−H carboxylation. *Nature* **2016**, *531*, 215−219.
(24) Frankhouser, A. D.; Kanan, M. W. Phase Behavior That Enables Solvent-Free Carbonate-Promoted Furoate Carboxylation. *J. Phys. Chem. Lett.* **2020**, *11*, 7544−7551.
(25) Dick, G. R.; Frankhouser, A. D.; Banerjee, A.; Kanan, M. W. A scalable carboxylation route to furan-2,5-dicarboxylic acid. *Green Chem.* **2017**, *19*, 2966−2972.
(26) Xiao, D. J.; et al. A closed cycle for esterifying aromatic hydrocarbons with CO2 and alcohol. *Nat. Chem.* **2019**, *11*, 940−947.
(27) Porter, T. M.; Kanan, M. W. Carbonate-promoted C−H carboxylation of electron-rich heteroarenes. *Chem. Sci.* **2020**, *11*, 11936−11944.
(28) Benzigar, M. R.; et al. Recent advances in functionalized micro and mesoporous carbon materials: synthesis and applications. *Chem. Soc. Rev.* **2018**, *47*, 2680−2721.
(29) Peng, S. S.; et al. Fabrication of ordered mesoporous solid super base with high thermal stability from mesoporous carbons. *Microporous Mesoporous Mater.* **2017**, *242*, 18−24.
(30) Anslyn, E. V. D.; Dennis, A. *Modern physical organic chemistry*; University Science Books, 2006; p 273.
(31) Li, C.; Frankhouser, A.; Kanan, M. Carbonate-Catalyzed Reverse Water-Gas Shift to Produce Gas Fermentation Feedstocks for Renewable Liquid Fuel Synthesis. *ChemRxiv* **2021**.
(32) Wang, J.; Wu, Y.; Shi, Z.; Wu, C. Mesoporous carbon with large pore volume and high surface area prepared by a co-assembling route for Lithium-Sulfur Batteries. *Electrochim. Acta* **2014**, *144*, 307−314.
(33) Lee, H. I.; et al. Rational Synthesis Pathway for Ordered Mesoporous Carbon with Controllable 30- to 100-Angstrom Pores. *Adv. Mater.* **2008**, *20*, 757−762.
(34) Jun, S.; et al. Synthesis of New, Nanoporous Carbon with Hexagonally Ordered Mesostructure. *J. Am. Chem. Soc.* **2000**, *122*, 10712−10713.
(35) Chen, D.; Huang, F.; Cheng, Y.-B.; Caruso, R. A. Mesoporous Anatase TiO2 Beads with High Surface Areas and Controllable Pore Sizes: A Superior Candidate for High-Performance Dye-Sensitized Solar Cells. *Adv. Mater.* **2009**, *21*, 2206−2210.
(36) Goertzen, S. L.; Thériault, K. D.; Oickle, A. M.; Tarasuk, A. C.; Andreas, H. A. Standardization of the Boehm titration. Part I. CO2 expulsion and endpoint determination. *Carbon* **2010**, *48*, 1252−1261.
(37) Oickle, A. M.; Goertzen, S. L.; Hopper, K. R.; Abdalla, Y. O.; Andreas, H. A. Standardization of the Boehm titration: Part II. Method of agitation, effect of filtering and dilute titrant. *Carbon* **2010**, *48*, 3313−3322.
(38) Boehm, H. P. Some aspects of the surface chemistry of carbon blacks and other carbons. *Carbon* **1994**, *32*, 759−769.
(39) Chao, B.; Konggidinata, M. I.; Lin, L.; Zappi, M.; Gang, D. D. Effect of carbon precursors and pore expanding reagent on ordered mesoporous carbon for resorcinol removal. *J. Water Process Eng.* **2017**, *17*, 256−263.
(40) Ahmad, Z. U.; Lian, Q.; Zappi, M. E.; Buchireddy, P. R.; Gang, D. D. Adsorptive removal of resorcinol on a novel ordered mesoporous carbon (OMC) employing COK-19 silica scaffold: Kinetics and equilibrium study. *J. Environ. Sci.* **2019**, *75*, 307−317.
(41) Kim, D. J.; Lee, H. I.; Yie, J. E.; Kim, S.-J.; Kim, J. M. Ordered mesoporous carbons: Implication of surface chemistry, pore structure and adsorption of methyl mercaptan. *Carbon* **2005**, *43*, 1868−1873.
(42) Shieh, W.-C.; Dell, S.; Repič, O. Nucleophilic Catalysis with 1,8-Diazabicyclo[5.4.0]undec-7-ene (DBU) for the Esterification of Carboxylic Acids with Dimethyl Carbonate. *J. Org. Chem.* **2002**, *67*, 2188−2191.

Recommended by ACS

Direct Air Capture and Integrated Conversion of Carbon Dioxide into Cyclic Carbonates with Basic Organic Salts
Marcileia Zanatta, Victor Sans, *et al.*
JUNE 23, 2023
ACS SUSTAINABLE CHEMISTRY & ENGINEERING
READ

Tailoring Carbon Deposits on a Single-Crystal Cobalt Catalyst for Fischer–Tropsch Synthesis without Further Reduction: The Role of Surface Carbon and Penetrating...
Chuan Qin, Mingyue Ding, *et al.*
JUNE 13, 2023
ACS CATALYSIS
READ

Clean Preparation of Formed Coke from Semi-coke by the Carbonated Consolidation Process
Zhengqi Guo, Siwei Li, *et al.*
JULY 17, 2023
ACS OMEGA
READ

Bifunctional Artificial Carbonic Anhydrase for the Integrated Capture and Electrochemical Conversion of CO_2
Oriol Gutiérrez-Sánchez, Tom Breugelmans, *et al.*
OCTOBER 05, 2022
ACS SUSTAINABLE CHEMISTRY & ENGINEERING
READ

Get More Suggestions >

https://doi.org/10.1021/acssuschemeng.2c06977
ACS Sustainable Chem. Eng. 2023, 11, 5876−5882